Solid State Communications 159 (2013) 49–54

Contents lists available at SciVerse ScienceDirect

Solid State Communications

journal homepage: www.elsevier.com/locate/ssc

The low-temperature properties of the spin-one Heisenberg antiferromagnetic chain with the single-ion anisotropy

Yuan Chen *, You Wu

Department of Physics, College of Physics and Electronic Engineering, Guangzhou University, Guangzhou 510006, China

ARTICLE INFO

Article history:
Received 26 October 2012
Received in revised form
7 December 2012
Accepted 10 January 2013
by P. Sheng
Available online 31 January 2013

Keywords:
C. Heisenberg antiferromagnetic chain
C. Single-ion anisotropy
D. Low-temperature properties
E. Self-consistent method

ABSTRACT

The one-dimensional spin-one Heisenberg antiferromagnet with the single-ion anisotropy is explored on the basis of the modified spin-wave theory. The ground-state and low-temperature properties of the system are obtained within the self-consistent method. It is shown that the single-ion anisotropy suppresses the quantum and thermal spin fluctuations. The temperature dependence of the magnon internal energy and specific heat exhibits the power-law form in the low-temperature region. The power exponents are dependent on the anisotropy. Our results agree quite well with the quantum Monte Carlo estimates the exact results and some experimental data.

© 2013 Elsevier Ltd. All rights reserved.

1. Introduction

The spin-wave theory for Heisenberg antiferromagnets (HAFMs) was initiated by Anderson [1] and extended by Kubo [2] more than half a century ago. But it is still one of the most powerful methods to study the low-temperature thermodynamics of Heisenberg magnets and still stimulates many researchers to further explorations. However, turning to low-dimensional HAFMs, the inadequacy of the conventional spin-wave theory (CSWT) is exposed by both numerically [3,4] and theoretically [5–8]. The CSWT accounts for the existence of long-range order; whereas the low-dimensional isotropic HAFM model is believed to have no long-range order in the ground-state [9]. When the CSWT [1,2] is used to study low-dimensional systems, it has to end up as a failure in diverging magnetization.

In order to overcome the thermodynamic divergence for CSWT, Takahashi formulated a modified spin-wave theory (MSWT) for low-dimensional Hensenberg ferromagnets [10] by constraining the magnetization of each site to be zero. His idea was developed and extended by Takahashi [11] and Hirsch and Tang [12] for two-dimensional HAFMs, and by Yamamoto and Fukui [13] for Heisenberg ferrimagnets spin chains. The MSWT can provide low-temperature results of low-dimensional spin systems in good agreement with other approaches and experiments. Recently, MSWT has been employed to investigate more complex systems, such as frustrated magnets [14–16] and random magnets [17–19]. Within the MSWT, the entanglement entropies [20], and the effect of spin–phonon coupling on the Haldane gap [21], and three-magnon processes in the dynamic structure factor [22], have been studied in the low-dimensional HAFMs, respectively.

Some different ways of implementing the MSWT for HATM, which lead to the improvement of MSWT, are currently found in the literature. For two-dimensional HATMs, Takahashi [11] and Hirsch and Tang [12] proposed the scheme, which suppresses the divergence of the sublattice magnetizations by introducing an ideal spin-wave density matrix (SWDM). Hereafter, we will refer to this scheme as SWDM. Yamamoto and Hori [23] introduced a slightly different strategy called full-diagonalization (FD) scheme, which diagonalizes the Hamiltonian keeping the dispersion relations free from temperature. Rocha-Filho et al. [24] developed these two different schemes to investigate the frustrated HAFM chain. Hauke et al. [25] extended Takahashi's MSWT to the spatially anisotropic triangular lattice by optimization of the ordering vector.

However, those schemes have to minimize the free energy in order to obtain the optimum thermal distribution function. Those schemes seem too complex to understand in the simple way. In this paper, our aim is to provide a simple self-consistent method for the one-dimensional HATM within the MSWT. Our approach is that we introduce a Lagrange multiplier in the Hamiltonian to keep zero sublattice magnetization. After the effective Hamiltonian is diagonalized, the Bose–Einstein distribution function is known. In the presence of the easy-axis single-ion anisotropy, the ground-

* Corresponding author. Tel./fax: +86 20 39366871.
E-mail address: newbayren@163.com (Y. Chen).

0038-1098/$ - see front matter © 2013 Elsevier Ltd. All rights reserved.
http://dx.doi.org/10.1016/j.ssc.2013.01.016

state and low-temperature thermodynamic properties of the system are found by determining the Lagrange multiplier under the mean of zero sublattice magnetization. By comparing our results with the quantum Monte Carlo (QMC) estimates, the exact-diagonalization (ED) results and the experimental data of TMNIN $[(C_2H_3)_4NNi(NO_2)_3]$ [26], our results are able to give the reliable information about magnetic properties of HAFM systems.

The rest of the paper is organized as follows: in Section 2, we rewrite the Hamiltonian in terms of bosonic operators by means of the Holstein–Primakoff transformation [27]. By introducing a Lagrange multiplier, an effective Hamiltonian is diagonalized by Bogoliubov transformation [28]. In Section 3, we discuss the effects of the single-ion anisotropy on the thermodynamic properties (such as the ground-state energy, internal energy, specific heat and magnetic susceptibility). We also compare the present method with the results of existing theories, numerical estimates and some available experimental data. Finally, the main points of the work are summarized in Section 4.

2. Model

Considering the one-dimensional spin-one HAFM model with the easy-axis single-ion anisotropy. Since the ground-state is a Néel-ordered state, we separate the lattice (with 2N sites) into two interpenetrating sublattice, where the sublattice A (B) is defined for the up (down) spins in the Néel-order state. The Hamiltonian can be written as

$$\mathcal{H}=\frac{1}{2}J\sum_{\langle ij\rangle}(S_{A_i}^{+}S_{B_j}^{-}+S_{A_i}^{-}S_{B_j}^{+})+J\sum_{\langle ij\rangle}S_{A_i}^{z}S_{B_j}^{z}-D\left(\sum_{i}(S_{A_i}^{z})^2+\sum_{j}(S_{B_j}^{z})^2\right), \tag{1}$$

where J is the nearest-neighbor exchange interaction ($J>0$), and D is a positive parameter and measures the strength of the single-ion anisotropy. The first summation runs over pairs of nearest-neighbor sites, the second and third ones over all sites of each sublattice. In Eq. (1), $S_i^{\pm}=S_i^x\pm iS_i^y$ are the spin raising and lowing operators. S_i^x, S_i^y and S_i^z represent the three components of the spin $S=1$ operator at site i.

By replacing the spins with boson creation and annihilation operators we can transform the spin problem to a more standard many-body interacting problem. This can be done by the Holstein–Primakoff transformation [27]

$$S_{A_i}^{+}=\sqrt{2-a_i^{+}a_i}a_i,\quad S_{A_i}^{-}=a_i^{+}\sqrt{2-a_i^{+}a_i},\quad S_{A_i}^{z}=1-a_i^{+}a_i \tag{2}$$

for the spins in sublattice A and

$$S_{B_j}^{+}=b_j^{+}\sqrt{2-b_j^{+}b_j},\quad S_{B_j}^{-}=\sqrt{2-b_j^{+}b_j}b_j,\quad S_{B_j}^{z}=b_j^{+}b_j-1 \tag{3}$$

in the sublattice B. Here (a^{+},b^{+}) and (a,b) are the creation and annihilation operators of spin deviations. By use of the Holstein–Primakoff transformation, we obtain the approximate Hamiltonian in powers of $a_i^{+}a_i$ or $b_j^{+}b_j$.

The CSWT naively diagonalizes this approximate Hamiltonian and ends up with the number of bosons diverging with increasing temperature. A very important modification to the CSWT is the constraint of zero staggered magnetization [11,12]

$$\sum_i S_{A_i}^{z}-\sum_j S_{B_j}^{z}=0$$

introduced in MSWT. In the SWDM scheme [11], the ideal spin-wave density matrix is introduced with both the Fourier transformation

$$a_i=\frac{1}{\sqrt{N}}\sum_k e^{\mathbf{ik}\cdot\mathbf{R}_i}a_k, \tag{4}$$

$$b_j=\frac{1}{\sqrt{N}}\sum_k e^{-\mathbf{ik}\cdot\mathbf{R}_j}b_k \tag{5}$$

and the Bogoliubov transformation [28]

$$a_k=\cosh\theta_k\alpha_k+\sinh\theta_k\beta_k^{+}, \tag{6}$$

$$b_k=\cosh\theta_k\beta_k+\sinh\theta_k\alpha_k^{+}. \tag{7}$$

Here N is the number of sites in each sublattice. Then the low-temperature thermodynamics are obtained after the free energy is minimized under the zero staggered magnetization.

In this paper, we take a slightly different procedure. In order to enforce the constraint of zero staggered magnetization

$$\sum_i(1-a_i^{+}a_i)-\sum_j(-1+b_j^{+}b_j)=0, \tag{8}$$

we introduce a Lagrange multiplier μ in the system. And then the Hamiltonian is rewritten as the effective Hamiltonian,

$$\mathcal{H}_{eff}=\mathcal{H}-\mu\left[\sum_i(1-a_i^{+}a_i)-\sum_j(-1+b_j^{+}b_j)\right] \tag{9}$$

and let

$$\mu=(2J+D)(\lambda-1). \tag{10}$$

By use of the transformations [i.e. Eqs. (2)–(7)] in Eq. (10) and keeping only the leading terms we obtain the approximate Hamiltonian

$$\mathcal{H}_{eff}=E_{GS}+\sum_k\omega_k(\alpha_k^{+}\alpha_k+\beta_k^{+}\beta_k)+\sum_k\xi_k(\alpha_k\beta_k+\alpha_k^{+}\beta_k^{+}) \tag{11}$$

in the reciprocal space. Since A and B sublattices are introduced in this system, the sum in Eq. (11) is over the reduced Brillouin zone which contains N wave vectors $\mathbf{k}$.

The effective Hamiltonian $\mathcal{H}_{eff}$ can be diagonalized by imposing the coefficient ξ_k to be zero. Then, $\mathcal{H}_{eff}$ is given by

$$\mathcal{H}_{eff}=E_{GS}+\sum_k\omega_k(\alpha_k^{+}\alpha_k+\beta_k^{+}\beta_k), \tag{12}$$

where E_{GS} whose zero-temperature value denotes the ground-state energy, and the dispersion relation ω_k is given by, respectively

$$E_{GS}=-2N(J+D)-N(2J+D)(2\lambda-1)+\sum_k\omega_k, \tag{13}$$

$$\omega_k=\sqrt{(2J+D)^2\lambda^2-(2J\cos k)^2}. \tag{14}$$

In Eq. (12), the occupation number operators, $\alpha_k^{+}\alpha_k$ and $\beta_k^{+}\beta_k$, account for two degenerate spin-wave branches of HAFM. Therefore, their expectation values are the Bose–Einstein distribution functions

$$n_k=\langle\alpha_k^{+}\alpha_k\rangle=\langle\beta_k^{+}\beta_k\rangle=(e^{\omega_k/T}-1)^{-1}. \tag{15}$$

The mean of zero staggered magnetization is obtained by using the thermal average

$$\langle\cdots\rangle\equiv\frac{\mathbf{Tr}[\ldots e^{-\mathcal{H}_{eff}/T}]}{\mathbf{Tr}[e^{-\mathcal{H}_{eff}/T}]}$$

in Eq. (8). Here T is the temperature. Then λ is self-consistently determined by

$$\frac{1}{N}\sum_k\frac{(2J+D)\lambda}{\omega_k}(2n_k+1)=3. \tag{16}$$

Thus, we obtain the set for λ, ω_k and n_k, as seen in Eqs. (14)–(16). If the parameter λ is solved by the set of equations, we know the ground-state and low-temperature properties, such as the ground-state energy E_{GS} and the specific heat c.

3. Results and discussions

First, we analyze the anisotropy dependence of the ground-state energy E_{GS}. At zero temperature, the Bose–Einstein distribution function yields $n_k = 0$. Then using Eqs. (13) and (16) at $T=0$, we can numerically evaluate the ground-state energy E_{GS} and the Lagrange multiplier λ. The effects of the single-ion anisotropy on the ground-state energy is shown in Fig. 1. The ground-state energy decrease with the increasing anisotropy D. In fact the results show that the quantum fluctuation is suppressed with increasing single-ion anisotropy. In the inset of Fig. 1, the decaying behavior of the reduced Lagrange multiplier λ is observed with increasing anisotropy D. At zero temperature, λ ensures the zero staggered magnetization.

In Table 1, the lattice size for the QMC estimation [29] is chosen to be $L = 9,17,25$ and 33, respectively. It can be seen that our values of E_{GS} are fitted better to those of the QMC data obtained from $L=25$. Noted that the characteristic length of the chain [29] is 14–17 and 18–24 for the anisotropy $D = 0.1,0.2$, respectively. The finite-size effect is significant for $L < 25$. In the isotropic case (i.e. $D=0$), the comparison with other methods is tabulated in Table 2. Liang [30] used ED to estimate the exact ground-state energy per site to be $-1.402J$ by using a 64-site linear chain. Our result for the isotropic case is in good agreement with the corresponding MSW (within FD scheme) result [15], QMC estimates [31] and ED result [30]. As shown in Table 2, our E_{GS} is better than those obtained from other theoretical methods such as the MSW (within SWDM scheme) [24] and perturbation (PB) [32] methods. Somewhat larger deviation of the coupled-cluster (CC) method [33] from the QMC value for E_{GS} is also found.

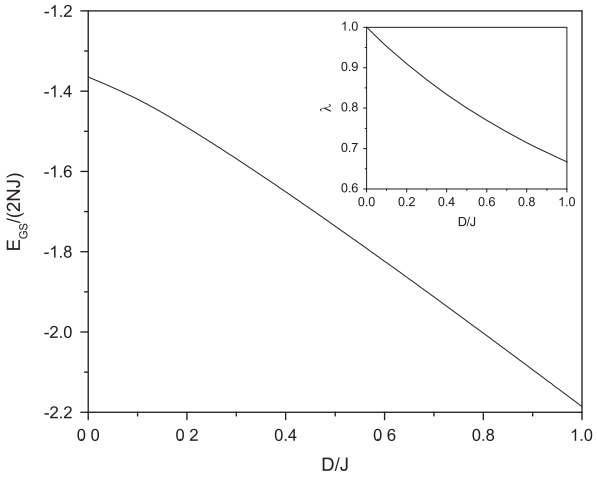

Fig. 1. Ground-state energy as a function of the single-ion anisotropy D in units of J. In the inset, the Lagrange multiplier λ is given as a function of D in units of J by using Eq. (16) at zero temperature.

Table 1
Ground-state energy per site in units of J compared with the QMC values [29] by using the chain length $L = 9,17,25$ and 33, respectively, for various D.

Anisotropy	Ours	$L=9$	$L=17$	$L=25$	$L=33$
$D/J=0.1$	−1.41675	−1.34244	−1.40025	−1.42196	−1.43394
$D/J=0.2$	−1.48889	−1.41722	−1.47335	−1.49508	−1.50536

Table 2
Ground-state energy per site compared with other methods for the one-dimensional isotropic ($D=0$) spin-1 HAFM. Here the exchange interaction takes $J=1$.

Ours	SWDM [24]	FD [15]	QMC [31]	ED [30]	PB [32]	CC [33]
−1.3645	−1.4901	−1.3946	−1.4015	−1.402	−1.3594	−1.3294

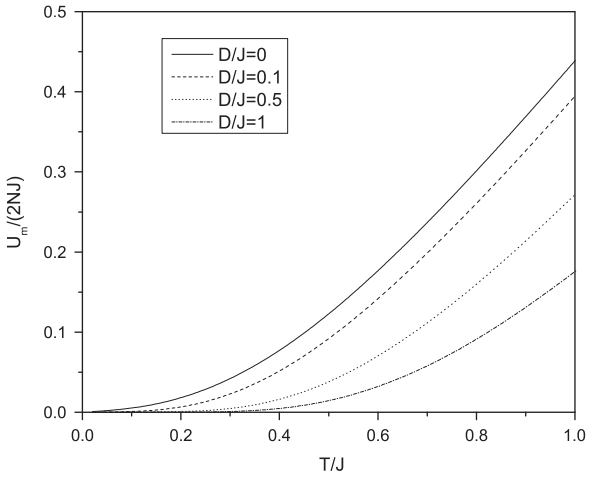

Fig. 2. The excitation energy U_m as a function of temperature.

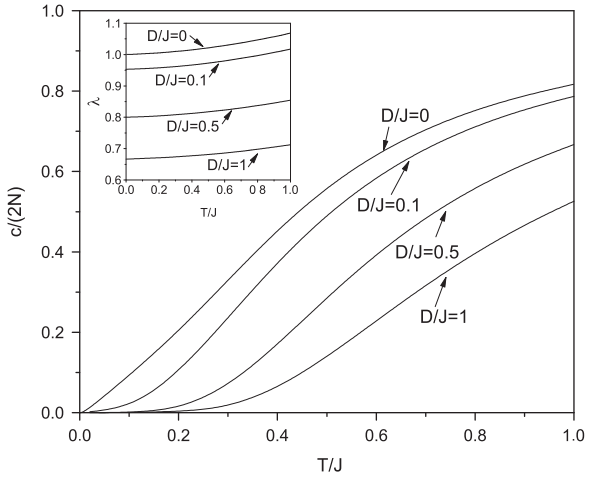

Fig. 3. The specific heat as a function of temperature. In the inset, the Lagrange multiplier λ is plotted as a function of temperature T for different anisotropy D.

Next we calculate the thermodynamic properties. The total internal energy $U = \langle \mathcal{H}_{eff} \rangle$ can be expressed as

$$U(T) = E_{GS} + 2\sum_k \omega_k n_k. \tag{17}$$

Then the excitation energy is given by $U_m = U(T) - E_{GS}(T=0)$. The magnon contribution to the average specific heat c is obtained by differentiating U with respect to the temperature T, i.e.

$$c = \frac{\partial U}{\partial T}. \tag{18}$$

Figs. 2 and 3 exhibit the variations of the magnon internal energy U_m and specific heat c with the temperature T and the single-ion anisotropy D, respectively. If D is fixed, U_m and c all increase with increasing T in the low-temperature region. As the temperature gets larger, the fluctuations due to the thermal motion of the spins are more intensive, and then this leads to the increase of

internal energy. It is noticed that U_m and c decrease with increasing D for a given T, which indicates that the fluctuation is suppressed with increasing anisotropy. To obtain the effects of the anisotropy on the Lagrange multiplier λ at non-zero temperatures, we plot λ as a function of temperature T for different anisotropy D, as seen in the inset of Fig. 3. It is found that λ increases with increasing T for D given. If the temperature T is fixed, λ increases with decreasing D, which is similar to the zero-temperature case.

Fig. 4 shows the variation of the total internal energy with temperature for the one-dimensional isotropic HAFM. We compare our values for the isotropic case with the QMC [34] and the second-order Green's function theory (GFT) [35] results. In the low-temperatures $0 < T/J < 2$, GFT fails to give more reliable results. In this region our curve gets closer to the QMC curve.

The temperature dependence of the specific heat is shown in Fig. 5 for the isotropic ($D=0$) HAFM chain. Our values are compared with those obtained by QMC [34], SGT [35] and Schwinger-boson mean field theory (SBMFT) [36]. Our calculated results show good agreement with the QMC values within the range $0 < T/J < 0.5$ where the spin-wave theory holds good. When the temperature is very low, our method works better than SBMFT and GFT for our results are closer to the high accurate QMC data. As shown in Fig. 5, our scheme has some advantages over the SWDM scheme.

In the following, we consider the power-law behavior of the magnon internal energy $U_m(T)$ and specific heat $c(T)$. In Figs. 6 and 7, we make a logarithmic plot of $U_m(T)$ and $c(T)$ as a function of T in order to elucidate its low-temperature behavior. If a simple power-law behavior is to be found, it will not be in the region very close to $T=0$ but for values of T such that k_BT is greater than the gap energy [26,37]. The numerical estimate for the gap energy for the one-dimensional HAFM, with spin 1, the energy gap is $0.4105J$ [21,26]. We find that $U_m(T)$ and $c(T)$ indeed exhibit an initial power-law behavior, $U_m(T) \sim T^{\alpha}$ and $c(T) \sim T^{\beta}$ in the low-temperature region $0.4 \le T/J \le 0.7$.

As shown in Table 3, the exponents α and β depend on the single-ion anisotropy. α and β increase with increasing D. The stronger the anisotropy (i.e. larger D), the larger the exponents α and β. It indicates that the magnon internal energy and specific heat with larger anisotropy increase more rapidly at low-temperatures than those with smaller anisotropy parameter. For the $S=1$ isotropic ($D=0$) case, $\alpha = 2.0982$ and $\beta = 1.0326$, which is in agreement with the calculations of Bonner and Fisher's theoretical value ($\alpha = 2$, $\beta = 1$) [38], the numerical values ($\alpha = 2.06 \pm 0.03$) [38] and

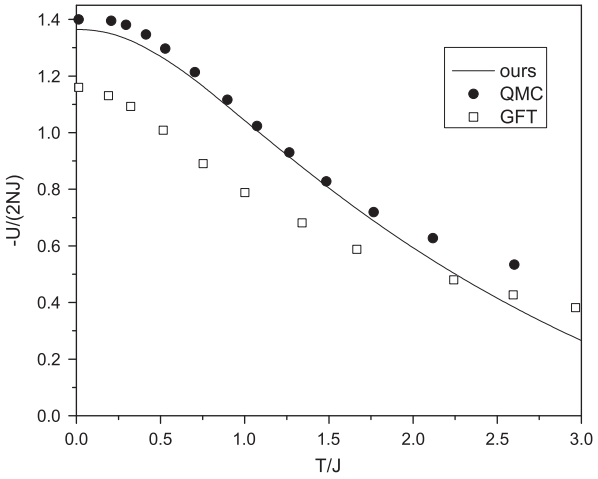

Fig. 4. Variation of the total internal energy with temperature for the one-dimensional isotropic ($D=0$) HAFM. The solid line is for the present calculation. Our values are compared with those from the QMC [34] and GFT [35].

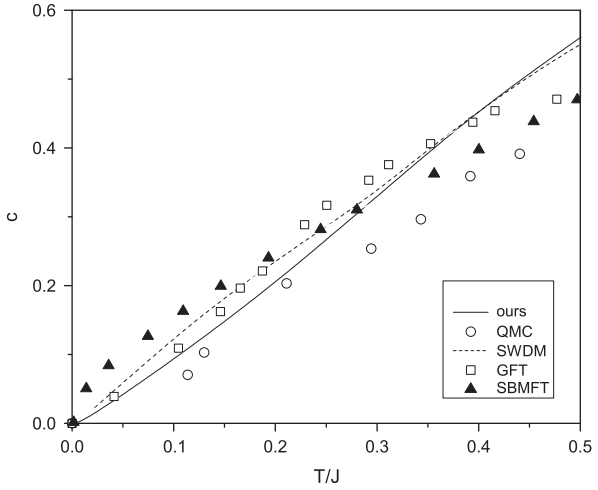

Fig. 5. The isotropic ($D=0$) specific heat as a function of temperature for the one-dimensional HAFM. The solid line is for the present calculation. Our results are compared with those from the QMC [34], GFT [35] and SBMFT [36].

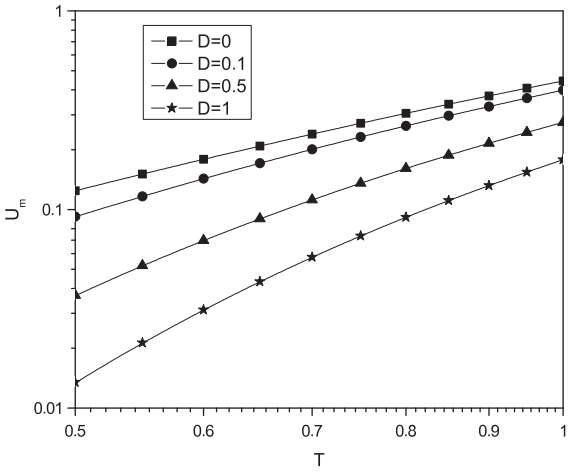

Fig. 6. The log–log plot of U_m versus T for various values of D. Here the exchange interaction takes $J=1$.

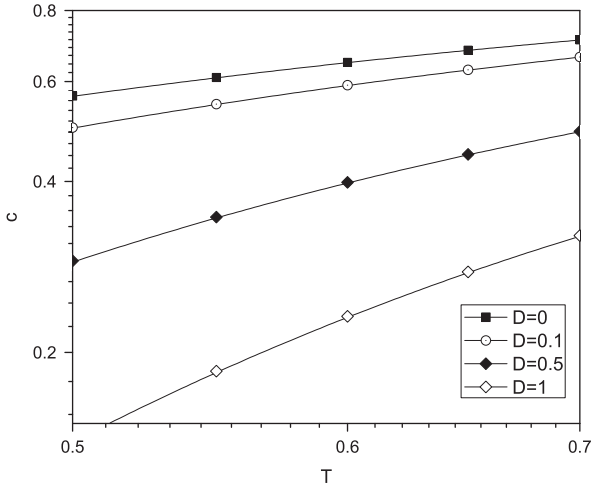

Fig. 7. The log–log plot of c versus T for various values of D. Here the exchange interaction takes $J=1$.

Table 3
Values of exponents α and β for the $S=1$ one-dimensional HAFM when $D=0$, 0.1, 0.5 and 1, respectively. Here we choose the temperature range $0.35 \le T \le 0.65$ and take the exchange interaction $J=1$.

Exponents	$D=0$	$D=0.1$	$D=0.5$	$D=1$
α	2.0982	2.6586	4.0926	5.5216
β	1.0326	1.192	2.3206	3.6409

the QMC value ($\beta = 1.06275$) [34] and the SGT result ($\beta = 1.0104$) [35].

Finally, we will discuss the behaviors of the magnetic susceptibility at low-temperatures. The susceptibility per site, χ, is defined by [10,11,15]

$$\chi = \frac{1}{3T}\frac{1}{2N}(\langle M^2\rangle - \langle M\rangle^2), \tag{19}$$

where $M = \sum_i S^z_{Ai} + \sum_i S^z_{Bj}$. Due to the fact that the expectation values of occupation number operators yield $\langle \alpha_k^+ \alpha_k\rangle = \langle \beta_k^+ \beta_k\rangle$ in this paper, the total magnetization $\langle M\rangle$ vanishes. Then the magnetic susceptibility is rewritten as

$$\chi = \frac{1}{3T}\frac{1}{2N}\sum_{ij}\langle S_i^z S_j^z\rangle \tag{20}$$

through the z-component correlation function $\langle S_i^z S_j^z\rangle$. In Eq. (20) the sum runs over all sites of the lattice. S_i^z is S_{Ai}^z (or S_{Bi}^z) when its site i belongs to the sublattice A (or B). Using the Holstein–Primakoff transformation, $S_i^z S_j^z$ is involved into products of two and four bosonic operators. After the four-boson terms are decoupled by Wick's theorem, one find that the correlation function $\langle S_i^z S_j^z\rangle$ is given by

$$\langle S_i^z S_j^z\rangle = \left[\frac{1}{2N}\sum_k \frac{(2\tilde{J}+\tilde{D})\lambda}{\tilde{\omega}_k}(2\tilde{n}_k+1)e^{-i\mathbf{k}\cdot(\mathbf{R}_i-\mathbf{R}_j)}\right]^2 - \frac{1}{4}\delta_{ij} - \left[\frac{1}{2N}\sum_k \frac{2\tilde{J}\cos k}{\tilde{\omega}_k}(2\tilde{n}_k+1)e^{-i\mathbf{k}\cdot(\mathbf{R}_i-\mathbf{R}_j)}\right]^2 \tag{21}$$

via the Fourier and Bogoliubov transformations. Substituting Eq. (21) into Eq. (20), we find

$$\chi = \frac{1}{3TN}\sum_k \tilde{n}_k(\tilde{n}_k+1). \tag{22}$$

In the linear spin-wave approximation, $\tilde{J}=J$, $\tilde{D}=D$, $\tilde{\omega}_k=\omega_k$ and $\tilde{n}_k=n_k$. If the effective Hamiltonian $\mathcal{H}_{eff}$ [in Eq. (9)] contains products of four bosonic operators, the calculation becomes the first-order spin-wave approximation. In this case, all (J,D,ω_k,n_k) are replaced by $(\tilde{J},\tilde{D},\tilde{\omega}_k,\tilde{n}_k)$ in Eqs. (10)–(16). In the first-order approximation, $\tilde{J}$ and $\tilde{D}$ are given by

$$\tilde{J} = J\left[\frac{3}{2} - \frac{1}{2N}\sum_k \frac{(2\tilde{J}+\tilde{D})\lambda - 2\tilde{J}\cos^2 k}{\tilde{\omega}_k}\right], \tag{23}$$

$$\tilde{D} = D\left[3 - \frac{2}{N}\sum_k \frac{(2\tilde{J}+\tilde{D})\lambda}{\tilde{\omega}_k}\right]. \tag{24}$$

In the isotropic limit (i.e. $D=0$), it is well known [26] that the compound TMNIN $[(C_2H_3)_4NNi(NO_2)_3]$ is the isotropic realization of the HAFM chains. It is interesting to know which spin-wave approximation better works for the behavior of the magnetic susceptibility χ with increasing temperature. In order to compare our results with those of the experimental and QMC studies, in Fig. 8 we plot the susceptibility as a function of temperature for the one-dimensional isotropic HAFM. It is found that our results obtained by the linear spin-wave approximation are very close to that of the experimental data [26] on TMNIN. In the region

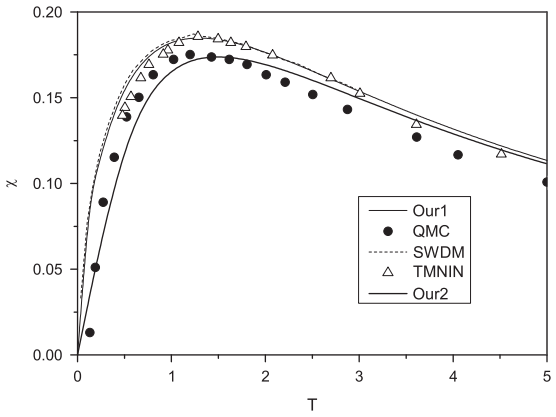

Fig. 8. The susceptibility as a function of temperature for the one-dimensional isotropic HAFM. The lines "Our1" and "Our2" are for the present calculation in the linear and first-order spin-wave approximation, respectively. "QMC", "TMNIN" and "SWDM" denote the QMC data [29] in the experimental result for TMNIN [26] and the result of MSWT within SWDM scheme [15], respectively. Here the exchange interaction takes $J=1$.

Table 4
Values of the magnetic susceptibility χ and Lagrange multiplier λ for the anisotropy $D=0.001$, 0.1 and temperature $T=0.3, 0.6, 1$, respectively. Those values are obtained in the first-order spin-wave approximation. Here the exchange interaction takes $J=1$.

Multiplier and susceptibility	λ			χ		
	$T=0.3$	$T=0.6$	$T=1$	$T=0.3$	$T=0.6$	$T=1$
$D=0.001$	1.0094	1.0284	1.0684	0.0892	0.1224	0.1405
$D=0.1$	0.9618	0.9799	1.0176	0.0026	0.0376	0.0899

$0 < T/J < 1.5$, our linear-approximation results are a little better than those obtained by the MSWT within the SWDM scheme [15]. For $T > 1.5J$, they coincide analytically. The isotropic results from our theory agree well with the QMC simulations [29]. In comparison to the QMC results, our results obtained by the first-order spin-wave approximation much better describe the behavior of χ than those obtained by the linear spin-wave approximation. It is because the susceptibility results from products of four bosonic operators. This means that the first-order approximation has some advantages over the linear approximation in the low-temperature thermodynamics.

It is shown in Table 4 and the inset of Fig. 3 that for the anisotropy D given, the higher the temperature, the larger the Lagrange multiplier λ, the larger the susceptibility χ. If T is fixed, one may observe that χ decreases with the increasing D. This occurs because the magnetic susceptibility measures the spin fluctuations which will be suppressed as the effects of anisotropy increase. It is obvious that the anisotropy D controls the magnitude of quantum fluctuations and stabilizes the Néel-phase.

4. Summary

Summarizing, we have investigated the one-dimensional $S=1$ antiferromagnet with the single-ion anisotropy by means of the modified spin-wave theory. Instead of introducing an ideal SWDM after a Bogoliubov transformation suggested by Takahashi [10], we adapt the self-consistent method to present the ground-state and low-temperature properties of the HAFM chain with single-ion anisotropy.

In the presence of the single-ion anisotropy D, the ground-state and low-temperature properties of the HAFM chain are

dependent of D. The ground-state energy, internal energy, specific heat and magnetic susceptibility are found to decrease with the increasing D. This is because that the quantum and thermal spin fluctuations are suppressed due to the anisotropy. The presence of the anisotropy tends to stabilize the two-sublattice Néel state. At low-temperatures, the excitation energy $U_m(T)$ and specific heat $c(T)$ increase with the increasing temperature which fit well by power laws, $U_m(T) \sim T^{\alpha}$ and $c(T) \sim T^{\beta}$, separately. The exponents are dependent on the anisotropy parameter. It is found that both α and β increase with the increasing anisotropy (i.e. larger D). In the isotropic case ($D = 0$), our results agree with the previous theoretical prediction, the numerical and the experimental results.

Our method gives an adequate description of the main features of the ground-state and low-temperature properties, keeping the computational effort at a minimum. From the above analysis, it can be seen that the ground-state and low-temperature properties of the system we are interested in are properly captured by this self-consistent method.

Acknowledgment

This is supported by the National Natural Science Foundation of China under Grant no. 10974059.

References

[1] P.W. Anderson, Phys. Rev. 86 (1952) 694.
[2] R. Kubo, Phys. Rev. 87 (1952) 568.
[3] R. Botet, J. Julien, M. Kolb, Phys. Rev. B 29 (1983) 5216.
[4] J.B. Parkinson, J.C. Bonner, G. Muller, M.P. Nightingale, H.W.J. Blote, J. Appl. Phys. 57 (1985) 3319.
[5] A. Moreo, Phys. Rev. B 35 (1987) 8562.
[6] D.P. Arovas, A. Auerbach, Phys. Rev. B 38 (1988) 316.
[7] T. Sakai, M. Takahashi, Phys. Rev. B 42 (1990) 1090.
[8] S.M. Rezende, Phys. Rev. B 42 (1990) 2589.
[9] N.D. Mermin, H. Wagner, Phys. Rev. Lett. 17 (1966) 1133.
[10] M. Takahashi, Phys. Rev. Lett. 58 (1987) 168.
[11] M. Takahashi, Phys. Rev. B 40 (1989) 2494.
[12] J.E. Hirsch, S. Tang, Phys. Rev. B 40 (1989) 4769.
[13] S. Yamamoto, T. Fukui, Phys. Rev. B 57 (1998) R14008.
[14] E.S. Pisanova, N.B. Ivanov, N.S. Tonchev, Phys. Rev. B 65 (2002) 212404.
[15] S. Yamamoto, Phys. Rev. B 69 (2004) 064426.
[16] N. Karchev, J. Phys. Condens. Matter 21 (2009) 056008.
[17] A.L. Chernyshev, Y.C. Chen, A.H. Castro Neto, Phys. Rev. B 65 (2002) 104407.
[18] X. Wan, K. Yang, R.N. Bhatt, Phys. Rev. B 66 (2002) 014429.
[19] E.V. Castro, N.M.R. Peres, K.S.D. Beach, Anders.W. Sandvik, Phys. Rev. B 73 (2006) 054422.
[20] H.F. Song, N. Laflorencie, S. Rachel, K. Le Hur, Phys. Rev. B 83 (2011) 224410.
[21] M.E. Gouvêa, A.S.T. Pires, Phys. Rev. B 75 (2007) 052401.
[22] L.S. Lima, A.S.T. Pires, Solid State Commun. 148 (2008) 541.
[23] S. Yamamoto, H. Hori, J. Phys. Soc. Jpn 72 (2003) 769.
[24] G.M. Rocha-Filho, A.S.T. Pires, M.E. Gouvêa, Eur. Phys. J. B 56 (2007) 7.
[25] P. Hauke, T. Roscilde, V. Murg, J.I. Cirac, R. Schmied, New J. Phys. 12 (2010) 053036.
[26] V. Gadet, M. Verdaguer, V. Briois, A. Gleizes, J.P. Renard, P. Beauvillain, C. Chappert, T. Goto, K. Le Dang, P. Veillet, Phys. Rev. B 44 (1991) 705.
[27] H. Holstein, H. Primakoff, Phys. Rev. 59 (1940) 1098.
[28] N.N. Bogoliubov, J. Phys. (USSR) 11 (1947) 23.
[29] S. Yamamoto, S. Miyashita, Phys. Rev. B 50 (1994) 6277.
[30] S. Liang, Phys. Rev. Lett. 64 (1990) 1597.
[31] S. Todo, K. Kato, Phys. Rev. Lett. 87 (2001) 047203.
[32] D.L. Bullock, Phys. Rev. A 137 (1965) 1877.
[33] W.H. Wong, C.F. Lo, Y.L. Wang, Phys. Rev. B 50 (1994) 6126.
[34] S. Yamamoto, S. Miyashita, Phys. Rev. B 48 (1993) 9528.
[35] S.Q. Bao, Solid State Commun. 101 (1997) 193.
[36] Y.X. Li, B. Chen, Phys. Lett. A 374 (2010) 3514.
[37] S.J. Joshua, Aust. J. Phys. 37 (1984) 305.
[38] J.C. Bonner, M.E. Fisher, Phys. Rev. 135 (3A) (1964) A640.